Carbon Nanotube Enhanced Dynamic Polymeric Materials through Macromolecular Engineering

Erika B. Stopler[a,‡], Obed J. Dodo[a,‡], Alexander C. Hull[a], Kyle A. Weaver[a], Progyateg Chakma[a], Richard Edelmann[b], Logan Ranly[c], Mehdi B. Zanjani[c], Zhijiang Ye[c], Dominik Konkolewicz[a,*]

[a.] *Department of Chemistry and Biochemistry, Miami University, Oxford, OH 45056, USA.*
[b.] *Center for Advanced Microscopy & Imaging, Miami University, Oxford, OH 45056, USA.*
[c.] *Department of Mechanical and Manufacturing Engineering, Miami University, Oxford, OH 45056, USA.*
‡ *These authors contributed equally*
* *Correspondence: d.konkolewicz@miamiOH.edu*

Abstract

Dynamic covalent Diels-Alder chemistry was combined with multiwalled carbon nanotube (CNT) reinforcement to make strong, tough and conductive dynamic materials. Unlike other approaches to functionalizing CNTs, this approach uses Diels-Alder bonds between diene pendant groups on the polymer and the CNT surface πσ bonds acting as dienophiles. Experimental and simulation data align with the CNT reinforcement coming from dynamic covalent bonds between the matrix and the CNT surface. Addition of just 0.9 wt% CNTs can lead to almost 3-fold increase in strength and 6-7 order of magnitude increases in electrical conductivity, and materials with 0.45 w% CNT can have excellent strength, self-healing and conductivity.

Keywords: Carbon nanotube, RAFT polymerization, dynamic covalent bonding, thermoresponsive materials, nanoreinforcement, electrical conductivity.

Polymer materials have almost limitless applications, ranging from adhesives, through performance composites and biomaterials.[1, 2] Bulk polymeric materials generally fall into the classes of thermoplastic materials which are easily processed due to the absence of crosslinks, albeit with limited performance above a certain temperature. Alternatively, thermoset materials have excellent performance and strength at all temperatures due to the extensive crosslinking, although their (re)processability is challenging or non-existent. Dynamic bonds, are able to exchange either intrinsically or in response to external stimulus.[3] Therefore, polymer materials which contain dynamic bonds have the processability of thermoplastic materials with the strength imparted by linkers and crosslinks in thermosets. In particular, dynamic covalent bonds have seen substantial interest as linkers in polymeric materials due to their strong covalent bond character and their stimulus responsive nature.[3, 4] Diels-Alder (DA) reactions including those between furan and maleimide have received significant attention as thermoresponsive bonds and linkers in polymer materials.[5, 6] Nevertheless, polymer matrices alone have limited strength, functionality, and performance, which therefore encouraged the development of a method for utilizing nanocomposites to improve material by introducing a high performance nanoreinforcement.[7-9] Various nanoreinforcements have been used in dynamic polymeric materials including silica, superparamagnetic nanoparticles, graphene, and carbon nanotubes (CNTs).[9-13]

CNTs have received significant attention due to both their strength and also their electrical conductivity.[14, 15] Generally, introduction of CNTs into a polymer matrix increases mechanical strength, and dramatically boosts electrical conductivity, especially above the percolation threshold.[16, 17] CNTs have been introduced into dynamic polymer matrices in the literature, with examples of CNTs included in epoxy matrices and also vinyl

polymer matrices. However, to truly gain the benefit of a nanocomposite reinforcement, effective connection of the polymer to the matrix must be achieved. Traditionally, the surface of CNTs are modified to carboxylic acid groups though harsh acidic reactions, with complex synthetic steps that limit large scale applications.[18, 19] However, as highlighted by Chang and Liu the π-bonds in the CNTs can react through DA processes with both dienes (such as furans) and dienophiles (such as maleimides) allowing mild, simple, *in-situ* modification of the nanotube surface.[20] This chemistry was utilized by Barner-Kowollik et al. to reversibly modify carbon nanotube surfaces.[21-24]

In the past two decades, reversible deactivation radical polymerization (RDRP) processes have been developed and they allow polymer architecture to be precisely designed, with excellent tolerance to chemical functionality.[25] Reversible addition-fragmentation chain transfer (RAFT) polymerization is a RDRP technique with exceptional tolerance to chemical functionality and it can be performed under mild conditions.[26] Recently, Pramanika and Singha,[27] utilized RAFT to create polymers with pendant furan groups which could reversibly attach to the multiwalled CNT surface, while Lim et al.[28] used this approach to functionalize CNTs to improve their colloidal stability. However, to date the approaches developed have focused on using the innate DA chemistry of CNTs with small molecule or polymer containing dienes and dienophiles have focused on colloidal or nanoscale materials. However, detailed exploration of dynamic and self-healing bulk materials with the polymer matrix precisely engineered by RAFT are not well understood, nor has the concept of utilizing the intrinsic DA chemistry of CNTs been used to make bulk scale dynamic self-healing nanocomposites. This communication utilizes the ability of RAFT to control macromolecular architecture, thermoresponsive furan-maleimide (FMI) DA dynamic covalent bonding and CNT reinforcement to create strong

and dynamic bulk polymer materials. This work indicates that less than 1 wt% CNT loading is sufficient to lead to substantial increases in polymer materials performance and lead to strong and powerful polymer materials. The excellent performance is enabled by the reversible bonding of the excess furan groups to the CNT surface,[20] enabling facile and responsive bonding of the polymer matrix to the nanoscale reinforcement. Due to the thermoresponsive FMI units, the materials have excellent dynamic character as assessed through self-healing experiments. The advantage of the CNT based nanoscale reinforcement strategy is to enhance mechanical, thermal and electrical properties of the RAFT based materials while maintaining dynamic properties imparted by the DA networks.

Well defined primary chain polymers were synthesized by RAFT polymerization, using ethyl acrylate (EA) as the main backbone forming monomer EA polymers have low glass transition temperatures, facilitating dynamic exchange under all conditions. Furfuryl methacrylate (FMA) was used to introduce the diene groups needed for dynamic covalent DA chemistry, and ethyleneglycol dimethacrylate (EGDMA) was used as a static branching point. Control materials without the dynamic covalent DA units were synthesized using glycidyl methacrylate (GMA) which can form crosslinks by epoxide ring opening, without introducing substantial dynamic character to the material, or bonding to the CNT surface. All RAFT polymerizations were performed using 2-(propionic acid)yl dodecyl trithiocarbonate (PADTC) as the chain transfer agent. A typical polymer synthesis is given in **Scheme 1a**. Branching can be introduced by adding 1 equivalent of EGDMA, with an otherwise identical polymerization process. The polymers were subsequently crosslinked using 1,1'-(methylenedi-4,1-phenylene)bismaleimide (BMI), since the polymer's pendant furan groups can react with the maleimide functionality as shown in **Scheme 1b**. The system will have an excess of furan groups, due to the 95% purity of the obtained BMI,[29]

allowing the excess furan to react with the CNT surface through DA chemistry, as highlighted in pink on **Scheme 1b**.

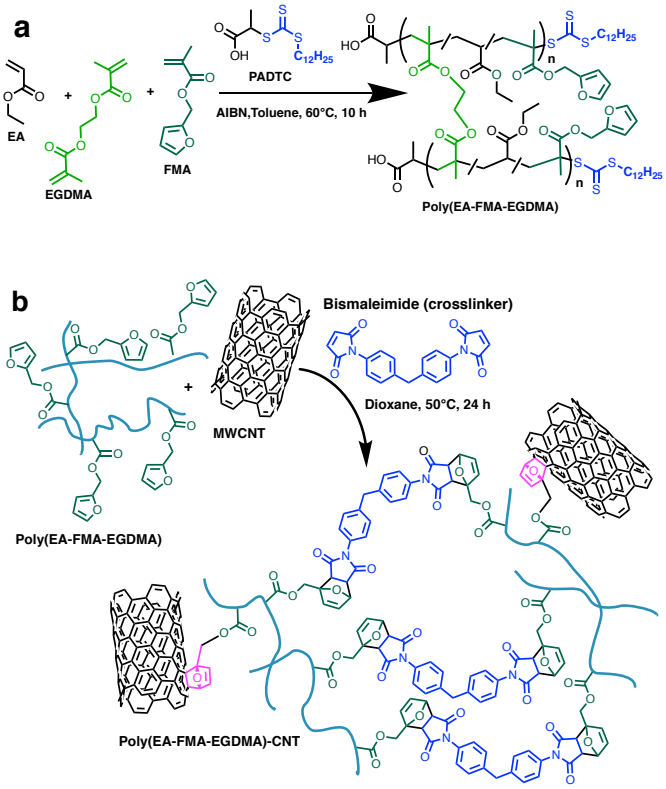

Scheme 1. a) RAFT polymerization of EA with FMA and EGDMA to give primary polymer bearing pendant furan group. b) Crosslinking of polymer with BMI in the presence of CNTs to give CNT dynamic material composites.

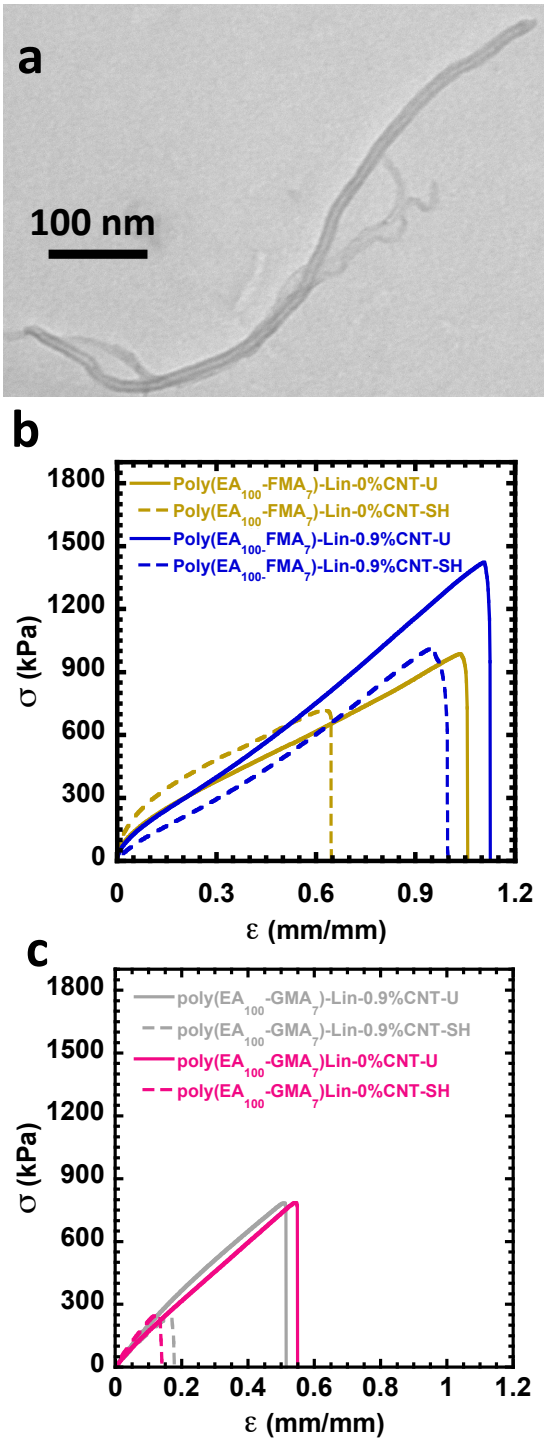

Figure 1. a) TEM micrograph of typical Carbon Nanotube used in this study. b) Stress strain curve of Poly(EA_{100}-FMA_7)-Lin uncut and 24 h healed at 75 °C materials, including materials

with and without 0.9 wt% CNT. c) Stress strain curve of Poly(EA_{100}-GMA_7)-Lin uncut and 24 h healed at 75 °C materials, including materials with and without 0.9 wt% CNT.

Figure 1a shows a TEM micrograph of a multiwalled CNTs used in this project. **Figure S1** includes TEM images of CNTs at lower magnification. There is variability in size to the tubes as is expected for non-fractionated CNT materials. Poly(EA) chains were synthesized with primary chain lengths of *ca*. 100 units of EA and either 7% or 4.5% crosslinker. The polymers are denoted as poly(EA_{100}-FMA_x)-Lin for a linear polymer containing x units of FMA, poly(EA_{100}-FMA_x)-Br for a branched polymer containing x units of FMA and poly(EA_{100}-GMA_x)-Lin for a linear polymer containing x units of GMA. Conversion and characterization data for these polymers are given in Table S1, with the molecular weight distributions, as determined by size exclusion chromatography (SEC), given in **Figure S2**. The clear advantage of RAFT over conventional polymerization is the ability to control the primary chain length, branching degree by addition of EGDMA and content of crosslinkers. Linear polymers were relatively well defined, while branched polymers had a significantly broader molecular weight distribution as seen in **Figure S2**.

Table 1: Mechanical and thermal properties of unreinforced and CNT reinforced materials.

Polymer	Wt% CNT	T_g (°C)	σ_{peak} (MPa)	ε_{break} (mm/mm)	Y (MPa)
poly(EA_{100}-FMA_7)-Lin	0	5	1.1±0.1	1.1±0.1	2.0±0.2
poly(EA_{100}-FMA_7)-Lin	0.9	-1	1.29±0.06	0.9±0.08	1.8±0.3
poly(EA_{100}-GMA_7)-Lin	0	-5	0.83±0.04	0.59±0.04	1.80±0.03
poly(EA_{100}-GMA_7)-Lin	0.9	-6	0.77±0.01	0.52±0.01	2.09±0.05
poly(EA_{100}-FMA_7)-Br	0	-1	1.03±0.06	0.81±0.03	2.3±0.2
poly(EA_{100}-FMA_7)-Br	0.225	2	1.32±0.09	0.94±0.03	2.46±0.09

poly(EA_{100}-FMA_7)-Br	0.45	2	2.2±0.3	0.79±0.04	5.6±0.7
poly(EA_{100}-FMA_7)-Br	0.9	4	3.2±0.3	0.75±0.05	9±1
poly(EA_{100}-$FMA_{4.5}$)-Br	0	-5	0.25±0.02	1.22±0.06	0.311±0.002
poly(EA_{100}-$FMA_{4.5}$)-Br	0.9	-5	0.54±0.05	0.97±0.08	0.66±0.03

After crosslinking the RAFT synthesized furan containing polymers using BMI polymer network materials were obtained. GMA was crosslinked by ring opening using N,N'-dimethylethylenediamine. These were synthesized both with and without CNT reinforcements. The typical morphology of a material with and without CNT reinforcement was explored using scanning electron microscopy (SEM) in **Figure S3**. The SEM images suggest that the majority of the materials with and without CNTs have similar morphologies (**Figure S3A** and **Figure S3B**), although there are certain domains with higher densities of CNTs and this may be due to the dispersion of CNT during synthesis. (**Figure 3C**). However, the vast majority of the materials have similar morphologies and the CNTs are visibly dispersed throughout the structure (**Figure 3B**).

Each material was characterized by tensile testing, infrared spectroscopy (IR), differential scanning calorimetry (DSC) and Dynamic Mechanical Analysis (DMA). Typical IR spectra are given in **Figure S4** with assignment given in **Table S2**. Interestingly the material in **Figure S4** containing 0.9 wt% CNTs had stronger absorbance in the alkene stretching region from 1600-1500 cm^{-1} and a stronger absorbance attributed to the addition of π-bonds from the CNTs. The difference is small due to the loading of CNTs being <1 wt%. The slightly stronger absorbance near 1651 cm^{-1} could be due to the DA adduct of furan groups to the CNT surface,[20] although the low mass fraction of CNTs limits conclusive assignment.

Glass transition temperatures were obtained by DSC and are reported in Table 1 with a typical DSC curve given in **Figures S5**. All glass transition temperatures were close to 0 °C, implying that all materials will be soft at room temperature. Each material was subjected to thermogravimetric analysis (TGA), with the TGA degradation profile given in **Figure S6**. Each material had a similar degradation profile with the onset of degradation occur in the range of 320-340 °C. This is most likely due to the bulk of each material being poly(EA). Typical tensile curves are given in **Figures S7-S16**, with average strain at break (ε_{break}), peak stress (σ_{peak}) given in **Table 1**.

Initially 0.9 wt% CNTs were utilized to determine if even a small CNT loading (<1 wt%) could give rise to powerful enhancements in materials electrical and mechanical properties. **Figure 1b** indicates that 0.9 wt% CNTs were sufficient to lead to noticeable strengthening of the poly(EA_{100}-FMA_7)-Lin material along with an increase in toughness. As seen in **Figure 1c**, 0.9 wt% CNT loading made negligible difference to the mechanical properties of poly(EA_{100}-GMA_7)-Lin control materials crosslinked with the GMA linker which should have minimal dynamic character, and negligible ability to attach to the CNT surface.

The difference between the mechanical properties of the poly(EA_{100}-GMA_7)-Lin control and the poly(EA_{100}-FMA_7)-Lin material is most likely due to the furan units in the poly(EA_{100}-FMA_7)-Lin material attaching to the surface of the nanotubes, and allowing efficient load transfer between the matrix and the CNT reinforcement. In contrast, the poly(EA_{100}-GMA_7)-Lin material cannot bind efficiently to the nanotubes through DA chemistry, and therefore load transfer is likely poorer between the matrix and the reinforcement. Therefore, the comparison of the DA active poly(EA_{100}-FMA_7)-Lin material which can bind the matrix covalently to the nanotubes and control material , the poly(EA_{100}-GMA_7)-Lin which cannot efficiently bind to the nanotubes highlight the importance of

enabling binding of the polymer matrix to the CNT surface. In the absence of covalent bonding between the matrix and the reinforcement, the nanotubes are unable to effectively have the load transferred to them as only sterics connect the matrix to the CNT.

The presence of thermoresponsive FMI adducts led to effective self-healing after heating to 75 °C for 24h for the poly(EA_{100}-FMA_7)-Lin materials both with and without CNTs, while much poorer recovery of mechanical properties was observed in the of poly(EA_{100}-GMA_7)-Lin control materials. The non-zero recovery of poly(EA_{100}-GMA_7)-Lin control materials can be attributed to the small number of H bonding units introduced after ring opening of the epoxide in GMA by the diamine.[30] Additionally, the CNT containing materials had superior electrical conductivity. The materials without added CNTs had no measurable conductivity, with estimated conductivity (κ) of $10^{-9} \pm 10^{-9}$ S/m based on literature reported conductivities of related polymers of poly(methyl methacrylate) which is an isomer of poly(EA) and poly(ethyl methacrylate) which has one added methyl group.[31, 32] In contrast the poly(EA_{100}-FMA_7)-Lin material had $\kappa = (1.0 \pm 0.7)\times10^{-2}$ S/m and poly(EA_{100}-GMA_7)-Lin material had $\kappa = (5 \pm 2)\times10^{-2}$ S/m. These represent 6-7 order of magnitude improvements in electrical conductivity due to the presence of just 0.9 wt% CNT loading.

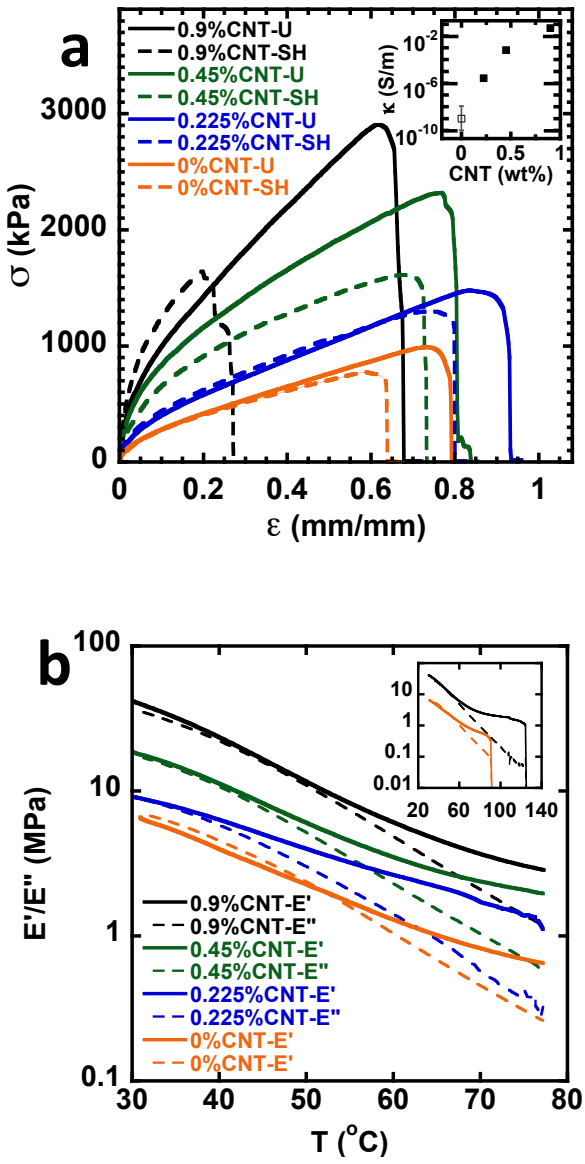

Figure 2: a) Typical stress (σ)-strain (ε) curves for both uncut (U) and self-healed (SH) Poly(EA_{100}-FMA_7)-Br materials with different loadings of CNT. Inset: Electrical conductivity (κ) vs CNT weight content in the material. b) Temperature sweep data for Poly(EA_{100}-FMA_7)-Br materials with different loadings of CNT. Inset shows full range of data for 0.9 and 0 wt% CNT loading.

Branching is a powerful parameter that can enhance material properties. Addition of 1 equivalent of divinyl monomer such as EGDMA can create highly branched polymers.[33] Interestingly the poly(EA_{100}-FMA_7)-Br materials synthesized with 1 equivalent of EGDMA to CTA, show remarkable enhancement in mechanical properties. Similar enhancement is observed in poly(EA_{100}-$FMA_{4.5}$)-Br, albeit starting from a weaker material at the lower crosslink density (**Table 1**). **Figure 2** and **Table 1** shows that with just 0.9 wt% of CNT loading, the peak stress in these materials is enhanced by a factor of 3 compared to the unreinforced materials. The conductivity of the poly(EA_{100}-FMA_7)-Br material with 0.9 wt% CNTs was $\kappa=(4.7 \pm 0.4)\times10^{-2}$ S/m.

As the nanotube loading is decreased to 0.45 and 0.225 wt% CNT, the extent of mechanical reinforcement and electrical conductivity is also decreased as demonstrated in **Figure 2a**. Importantly the data in **Figure 2a** indicates that all materials display self-healing characteristics. The very stiff 0.9 wt% loaded material had relatively little self-healing, while the 0.45 and 0.225 wt% CNT materials had relatively similar self-healing (SH) recovery compared to the uncut materials (U).

Due to the superior performance of the CNT reinforced materials based on poly(EA_{100}-FMA_7)-Br, all subsequent analysis focuses on these systems. A possible reason for the superior performance of the poly(EA_{100}-FMA_7)-Br compared to the linear equivalents, is that the branching can lead to an overall larger polymer chain with more FMA units. This could allow the matrix to better bridge and attach to multiple CNT reinforcements, enabling efficient load transfer in the polymer material. Electrical percolation, compared to mechanical reinforcement, is less impacted by chain bridging, which could explain why conductivity of the poly(EA_{100}-FMA_7)-Br, poly(EA_{100}-FMA_7)-Lin and poly(EA_{100}-

GMA_7)-Lin materials with 0.9 wt% CNTs is in the same order of magnitude, despite the superior mechanical properties of poly(EA_{100}-FMA_7)-Br.

Figure 2b shows the dynamic mechanical thermal analysis (DMTA) profiles over the range of 30 – 80 °C. The DMTA data show a thermal transition to a rubbery plateau followed by eventual disintegration of the material as the DA crosslinks dissociate. Interestingly, the inset to **Figure 2b** shows that poly(EA_{100}-FMA_7)-Br with 0.9 wt% CNTs can reach much higher temperatures before DA bond dissociation causes the material to fail compared to the poly(EA_{100}-FMA_7)-Br with 0 wt% CNTs. The higher storage modulus is also reflected in frequency sweep data in **Figure S17**. All materials had limited creep and good creep recovery as indicated in **Figure S18**. This is consistent with the DA units being essentially fixed at temperatures near ambient.

Finally, to confirm the impact of polymer-matrix-nanotube reinforcement molecular dynamics (MD) simulations were performed. MD simulations evaluated the mechanical properties of polymer matrix, polymer matrix with nanotubes, and matrix with covalent bonds between the nanotube and the matrix. A coarse-grained model for the polymers and cross-linkers[34] was used with polymer chains made up of 100 beads, interconnected through covalently bonded furan-maleimide crosslinkers. There are 7 linkers introduced per polymer chain to represent the 7% cross-linkers present in the experimental setup. Additionally, the CNTs were modelled as rigid cylinders formed by a number of beads (similar in size to the polymer beads) that provide a cylinder of 20 nm diameter. For simplicity and convenience of the model, the carbon nanotube length is set as equivalent to 200 bead diameters, and the number of carbon nanotubes (cylinders) in the simulation box is selected in a way to provide 0.9% of total mass of the system, comparable to the

experimental value. The crosslinker was based on furan-maleimide DA adducts developed earlier.[34] Simulation approach and a snapshot from the simulation is given in **Figure S19**.

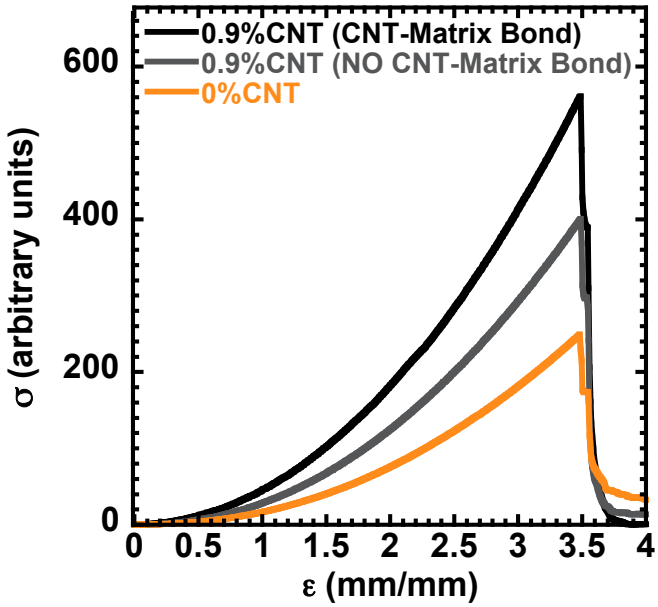

Figure 3: Simulated stress strain curve for polymer matrix containing primary chain lengths of 100, 7% furan groups. 95% of furan groups are crosslinked as part of the matrix. Orange curve is matrix only, grey is matrix with 0.9 wt% CNTs, with the CNTs dispersed but not bonded to the matrix, while black shows polymer matrix which is covalently bonded to the 0.9 wt% of CNTs.

As indicated in **Figure 3**, simulated stress-strain curve of the polymer matrix reaches an ε_{break} of *ca.* 3.5, with a σ_{peak} of ca. 250 a.u. Introduction of 0.9 wt% CNT led to a slight increase in peak stress, when the CNTs are not bonded to the matrix. Significant mechanical reinforcement is only realized with the presence of CNTs that are bonded to the matrix. This implies that the attachment of pendant furan-groups of the matrix need to be bonded to the CNTs to realize the substantial mechanical enhancements observed experimentally

in **Figure 1** and **2**. This is likely due to the covalent bonding between the matrix and the CNT leading to effective transfer of load between the matrix and the reinforcement.

In conclusion, a series of dynamic and self-healing polymer materials were synthesized and reinforced with multiwalled carbon nanotubes (CNTs). The use of dynamic covalent DA chemistry using furan and maleimides enabled self-healing polymer matrices and CNT composites. Experimental and simulation data suggest that the unreacted furan groups in the matrix are bonding to the CNT surface, leading to substantial enhancements in material strength and toughness. After introduction of just 0.9 wt% CNTs stress at break values can increase 2.7-fold to over 3 MPa, compared to the unreinforced materials in the branched matrices. In addition to mechanical reinforcement, electrical conductivity was dramatically increased by addition of CNTs.

SUPPLEMENTARY INFORMATION

Supplementary Information can be found online. Supplemental information includes supplemental experimental procedures, transmission electron microscopy, scanning electron microscopy, size exclusion chromatography, tensile testing data, infrared, differential scanning calorimetry and creep data

ACKNOWLEDGEMENTS

We greatly appreciate experimental assistance from Zachary Digby, Nethmi DeAlwis, Jeremy Via, Michael Duffy and Andre J Sommer. This material is based upon work supported by the National Science Foundation under Grant No. (DMR-1749730). Dominik Konkolewicz would also like to acknowledge support from the Robert H. and Nancy J. Blayney Professorship. The

authors acknowledge computational resources of the Ohio Supercomputer Center through Award PMIU0139.

AUTHOR CONTRIBUTIONS

The manuscript was written through contributions of all authors. All authors have given approval to the final version of the manuscript. ‡These authors contributed equally.

DECLARATION OF INTEREST

The authors declare no competing interest.

REFERENCES AND NOTES

1 S. Ramakrishna, J. Mayer, E. Wintermantel, K. W. Leong, *Compos Sci Technol* 2001, **61**, 1189.
2 M. A. C. Stuart, W. T. S. Huck, J. Genzer, M. Müller, C. Ober, M. Stamm, G. B. Sukhorukov, I. Szleifer, V. V. Tsukruk, M. Urban, F. Winnik, S. Zauscher, I. Luzinov, S. Minko, *Nat Mater* 2010, **9**, 101.
3 P. Chakma, D. Konkolewicz, *Angew Chem Int Ed* 2019, **58**, 9682.
4 W. Zou, J. Dong, Y. Luo, Q. Zhao, T. Xie, *Adv Mater* 2017, **29**, 1606100.
5 G. Hizal, U. Tunca, A. Sanyal, *J Polym Sci Part A: Polym Chem* 2011, **49**, 4103.
6 X. Chen, M. A. Dam, K. Ono, A. Mal, H. Shen, S. R. Nutt, K. Sheran, F. Wudl, *Science* 2002, **295**, 1698.
7 O. Breuer, U. Sundararaj, *Polym Compos* 2004, **25**, 630.
8 J. Jordan, K. I. Jacob, R. Tannenbaum, M. A. Sharaf, I. Jasiuk, *Mater Sci Eng: A* 2005, **393**, 1.
9 T. Engel, G. Kickelbick, *Polym Int* 2014, **63**, 915.
10 V. K. Thakur, M. R. Kessler, *Polymer* 2015, **69**, 369.
11 C. C. Corten, M. W. Urban, *Adv Mater* 2009, **21**, 5011.
12 X. Xiao, T. Xie, Y.-T. Cheng, *J Mater Chem* 2010, **20**, 3508.
13 Z. Spitalsky, D. Tasis, K. Papagelis, C. Galiotis, *Prog Polym Sci* 2010, **35**, 357.
14 N. Behabtu, C. C. Young, D. E. Tsentalovich, O. Kleinerman, X. Wang, A. W. K. Ma, E. A. Bengio, R. F. ter Waarbeek, J. J. de Jong, R. E. Hoogerwerf, S. B. Fairchild, J. B. Ferguson, B. Maruyama, J. Kono, Y. Talmon, Y. Cohen, M. J. Otto, M. Pasquali, *Science* 2013, **339**, 182.
15 M. M. Shokrieh, R. Rafiee, *Mech Compos Mater* 2010, **46**, 155.
16 W. Bauhofer, J. Z. Kovacs, *Compos Sci Technol* 2009, **69**, 1486.
17 J. N. Coleman, U. Khan, W. J. Blau, Y. K. Gun'ko, *Carbon* 2006, **44**, 1624.
18 P. Liu, *Eur. Polym. J.* 2005, **41**, 2693.
19 S. Bose, R. A. Khare, P. Moldenaers, *Polymer* 2010, **51**, 975.

20 C.-M. Chang, Y.-L. Liu, *Carbon* 2009, **47**, 3041.
21 N. Zydziak, C. M. Preuss, V. Winkler, M. Bruns, C. Hübner, C. Barner-Kowollik, *Macromol Rapid Commun* 2013, **34**, 672.
22 N. Zydziak, C. Hübner, M. Bruns, C. Barner-Kowollik, *Macromolecules* 2011, **44**, 3374.
23 B. Yameen, N. Zydziak, S. M. Weidner, M. Bruns, C. Barner-Kowollik, *Macromolecules* 2013, **46**, 2606.
24 N. Zydziak, C. Hübner, M. Bruns, A. P. Vogt, C. Barner-Kowollik, *Polymer Chemistry* 2013, **4**, 1525.
25 W. A. Braunecker, K. Matyjaszewski, *Prog Polym Sci* 2007, **32**, 93.
26 S. Perrier, *Macromolecules* 2017, **50**, 7433.
27 N. B. Pramanik, N. K. Singha, *RSC Adv* 2015, **5**, 94321.
28 C. M. Q. Le, X. T. Cao, Y. T. Jeong, K. T. Lim, *J. Ind. Eng. Chem.* 2018, **64**, 337.
29 Millipore-Sigma 1,1′-(Methylenedi-4,1-phenylene)bismaleimide Specification Sheet. https://www.sigmaaldrich.com/Graphics/COfAInfo/SigmaSAPQM/SPEC/22/227463/227463-BULK_____ALDRICH__.pdf (accessed Oct 27 2019).
30 B. Zhang, Z. A. Digby, J. A. Flum, P. Chakma, J. M. Saul, J. L. Sparks, D. Konkolewicz, *Macromolecules* 2016, **49**, 6871.
31 H. M. Kim, K. Kim, S. J. Lee, J. Joo, H. S. Yoon, S. J. Cho, S. C. Lyu, C. J. Lee, *Curr Appl Phys* 2004, **4**, 577.
32 C. A. Grimes, C. Mungle, D. Kouzoudis, S. Fang, P. C. Eklund, *Chem Phys Lett* 2000, **319**, 460.
33 B. Liu, A. Kazlauciunas, J. T. Guthrie, S. Perrier, *Macromolecules* 2005, **38**, 2131.
34 M. B. Zanjani, B. Zhang, B. Ahammed, J. P. Chamberlin, P. Chakma, D. Konkolewicz, Z. Ye, *Macromol Theory Simul* 2019, **28**, 1900008.

Graphical Abstract Table of Contents Entry